Editors' Suggestion | Featured in Physics

Evidence for a New Component of High-Energy Solar Gamma-Ray Production

Tim Linden,[1,*] Bei Zhou,[1,2,†] John F. Beacom,[1,2,3,‡] Annika H. G. Peter,[1,2,3,§] Kenny C. Y. Ng,[4,‖] and Qing-Wen Tang[5,1,¶]
[1]*Center for Cosmology and AstroParticle Physics (CCAPP), The Ohio State University, Columbus, Ohio 43210, USA*
[2]*Department of Physics, The Ohio State University, Columbus, Ohio 43210, USA*
[3]*Department of Astronomy, The Ohio State University, Columbus, Ohio 43210, USA*
[4]*Department of Particle Physics and Astrophysics, Weizmann Institute of Science, Rehovot 76100, Israel*
[5]*Department of Physics, Nanchang University, Nanchang 330031, China*

(Received 3 May 2018; revised manuscript received 23 July 2018; published 25 September 2018)

The observed multi-GeV γ-ray emission from the solar disk—sourced by hadronic cosmic rays interacting with gas and affected by complex magnetic fields—is not understood. Utilizing an improved analysis of the Fermi-LAT data that includes the first resolved imaging of the disk, we find strong evidence that this emission is produced by two separate mechanisms. Between 2010 and 2017 (the rise to and fall from solar maximum), the γ-ray emission was dominated by a polar component. Between 2008 and 2009 (solar minimum) this component remained present, but the total emission was instead dominated by a new equatorial component with a brighter flux and harder spectrum. Most strikingly, although six γ rays above 100 GeV were observed during the 1.4 yr of solar minimum, none were observed during the next 7.8 yr. These features, along with a 30–50 GeV spectral dip which will be discussed in a companion paper, were not anticipated by theory. To understand the underlying physics, Fermi-LAT and HAWC observations of the imminent cycle 25 solar minimum are crucial.

DOI: 10.1103/PhysRevLett.121.131103

The Sun is a bright source of multi-GeV γ rays, with emission observed both from its halo—due to cosmic-ray electrons interacting with solar photons—and its disk—due to hadronic cosmic rays (mostly protons) interacting with solar gas. (Emission from solar particle acceleration is bright only during flares and has not been observed above 4 GeV [1–8].) Although the halo emission [9] agrees with theory [10–12], the disk emission does not and hence is our focus.

Previously, the most extensive analysis of solar disk γ-ray emission was based on Fermi-LAT data from 2008 through 2014 [13] (for earlier work, see Refs. [9,14]), and it produced three results. First, the flux is bright, e.g., at 10 GeV, it exceeds the flux expected from Earth-directed cosmic rays interacting with the solar limb by a factor $\gtrsim$50 [15]. Second, it continues to 100 GeV, requiring proton energies $\sim$1000 GeV. Third, the 1–10 GeV flux is anticorrelated with solar activity, and it is $\sim$2.5$\times$ larger at solar minimum than solar maximum. [The "cycle 24" solar minimum approximately spanned 2007 through 2009. Fermi-LAT science observations (beginning in August, 2008) observed only the latter half of this period [16].] The *only* theoretical model of disk emission is the 1991 paper of Seckel, Stanev, and Gaisser (SSG) [17], which proposes that magnetic flux tubes can reverse incoming protons deep within the solar atmosphere, where they have an appreciable probability of producing outgoing γ rays. Though this enhances the γ-ray flux, the SSG prediction still falls a factor of $\sim$6 below the data at 10 GeV, and it does not explain the time variation.

In this and a companion paper, we perform new analyses of Fermi-LAT data based on a longer exposure (2008–2017), better data quality (Pass 8), and improved methods. In Ref. [18], we focus on the 1–100 GeV spectrum and its time variability. Compared to our earlier work [13], the flux is robustly detected up to 100 GeV, and the anticorrelation of the flux with solar activity is detected up to $\sim$30 GeV. Intriguingly, we discover a spectral dip between 30 and 50 GeV. This dip is unexpected and its origin is unknown. Here we extend Refs. [13,18] by going to higher energies, studying the time variation in a new way, and performing the first analysis of flux variations across the resolved solar disk. In the following, we detail our methodology, highlight key discoveries, and discuss possible theoretical implications.

The importance of this work is manifold. Because the disk γ-ray emission is brighter than expected, it motivates new searches with Fermi-LAT [19], the HAWC γ-ray experiment [20], and the IceCube neutrino observatory [21]. The results will yield valuable insights into the dynamic solar magnetic environment, from cosmic-ray modulation in the solar system to the fields deep within the photosphere. They will also advance searches for new physics [22–30]. Most generally, these searches provide the highest-energy data available to understand the Sun as an example of other stars.

Methodology.—We utilize Pass 8 SOURCE events from August 4, 2008, to November 5, 2017 (MET: 239557417–531557417), employing standard cuts. We include events exceeding 10 GeV observed within 0.5° of the solar center

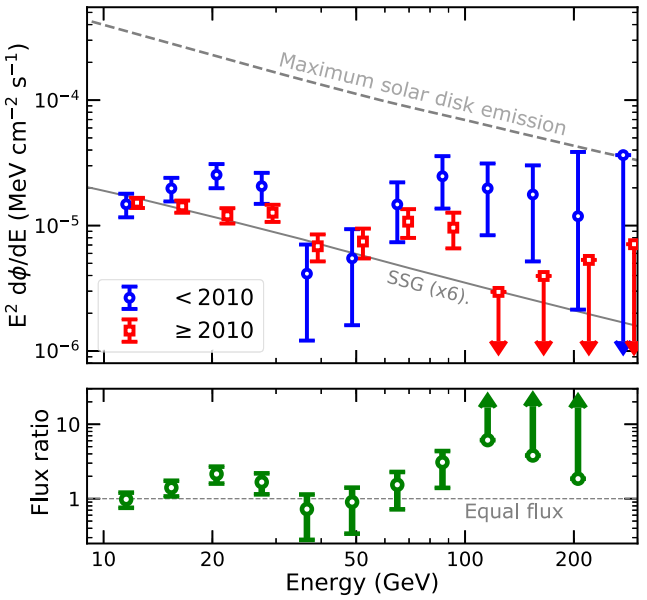

FIG. 1. (Top panel) The solar disk γ-ray spectrum during solar minimum (before January 1, 2010; blue circles) and after it (red squares). Small shifts along the x axis improve readability. The gray lines show the SSG model renormalized by a factor of 6 to fit the lowest-energy data point (solid line), and the maximum γ-ray flux that could be produced by hadronic cosmic rays (dashed line). (Bottom panel) The ratio of the γ-ray flux observed during and after solar minimum. All upper and lower limits are based on 2σ Poisson fluctuations in the photon count.

(the Sun's angular radius is 0.26°). The excellent angular resolution of >10 GeV γ rays minimizes the flux lost from our region of interest (ROI). In Appendix A of the Supplemental Material (SM) [31], we show that larger ROIs produce consistent results. We remove events observed when the Sun falls within 5° of the Galactic plane due to the larger diffuse background. This cut is smaller than in previous work but is sufficient due to the small ROI. We perform the first conversion of each γ ray to helioprojective coordinates utilizing SunPy [45] and astropy [46]. We ignore diffuse backgrounds, which we found in Ref. [18] to be negligible.

We calculate the Fermi-LAT exposure at the solar position in temporal bins of 5000 s (but use precise times for recorded events). Within this period, the Sun moves $<0.1°$ in the Fermi coordinate system, and the Fermi-LAT effective exposure is approximately constant. We assume a single exposure over the full ROI in each time bin, and we bin the exposure into 32 logarithmic energy bins spanning 10 GeV to 1 TeV. Because the Sun occupies a unique position in instrumental ϕ space, we calculate exposures calculated using ten independent ϕ bins. In Appendix B of the SM [31], we show that this ϕ dependence does not affect our results.

Flux, spectrum and time variation.—In Fig. 1, we show the solar γ-ray flux before and after January 1, 2010, which roughly corresponds to the end of the cycle 24 solar minimum. We note three key results. (a) The γ-ray flux significantly exceeds the SSG prediction (based on a proton interaction probability of 0.5%), in fact approaching the maximum allowed solar disk flux (for a detailed calculation, see Appendix E of the SM [31]). (b) The 30–50 GeV spectral dip, which we carefully examine in Ref. [18], is statistically significant both during and after solar minimum, though there is some evidence (2.5σ) that the dip deepens at solar minimum. Aside from the dip, the spectra in both time periods are significantly harder than predicted by SSG. (c) The strongest time variation is observed between solar minimum (largest flux) and the remaining solar cycle. At low energies this variation is moderate [13,14,18]. However, the amplitude increases with energy above 50 GeV, reaching a factor $\gtrsim 10$ above 100 GeV. None of these observations were anticipated by theory.

Morphology.—The large γ-ray flux suggests that a large fraction of the solar surface participates in γ-ray emission. To further elucidate the γ-ray generation mechanism(s), we resolve the γ-ray morphology across the solar surface. This reconstruction is possible at high ($\gtrsim 10$ GeV) energies due to the excellent ($\sim 0.1°$) Fermi-LAT angular resolution.

In Fig. 2, we show the location of γ rays in our analysis, dividing the data into two temporal bins (before and after January 1, 2010, corresponding to the end of the solar minimum) and two energy bins (below and above 50 GeV, corresponding to the spectral dip discussed in Ref. [18]). We find that, contrary to the SSG model, the emission is neither isotropic nor time invariant. Instead, it includes distinct polar and equatorial components, with separate time and energy dependences. In particular, it is apparent that γ rays above 50 GeV are predominantly emitted near the solar equatorial plane during solar minimum, but they are emitted from polar regions during the remaining cycle.

We utilize two separate methods to quantify the significance of this morphological shift. The first employs a Kolmogorov-Smirnov test to differentiate the distribution of γ rays in observed helioprojective latitude ($|T_y|$) during and after solar minimum. This method is model independent but loses sensitivity to convolving factors such as the instrumental point-spread function (PSF). Below 50 GeV, we find that the event morphologies are consistent to within 1.1σ. However, above 50 GeV, we reject the hypothesis that the latitude distributions during and after solar minimum are equivalent at 2.8σ. This provides reasonable evidence for a morphological shift.

Second, we define a two-component model of the solar surface, with equal-area equatorial and polar emission components (divided at $T_y = \pm 0.108°$). We fit the flux from each component, utilizing the angular reconstruction of each observed γ ray (see Appendix F of the SM [31]). This correctly accounts for the PSF but provides results that depend on the assumed emission model. In Appendix G of the SM [31], we show that different models produce similar results. This analysis provides two key results. (a) At all energies, the γ-ray emission becomes more polar after solar

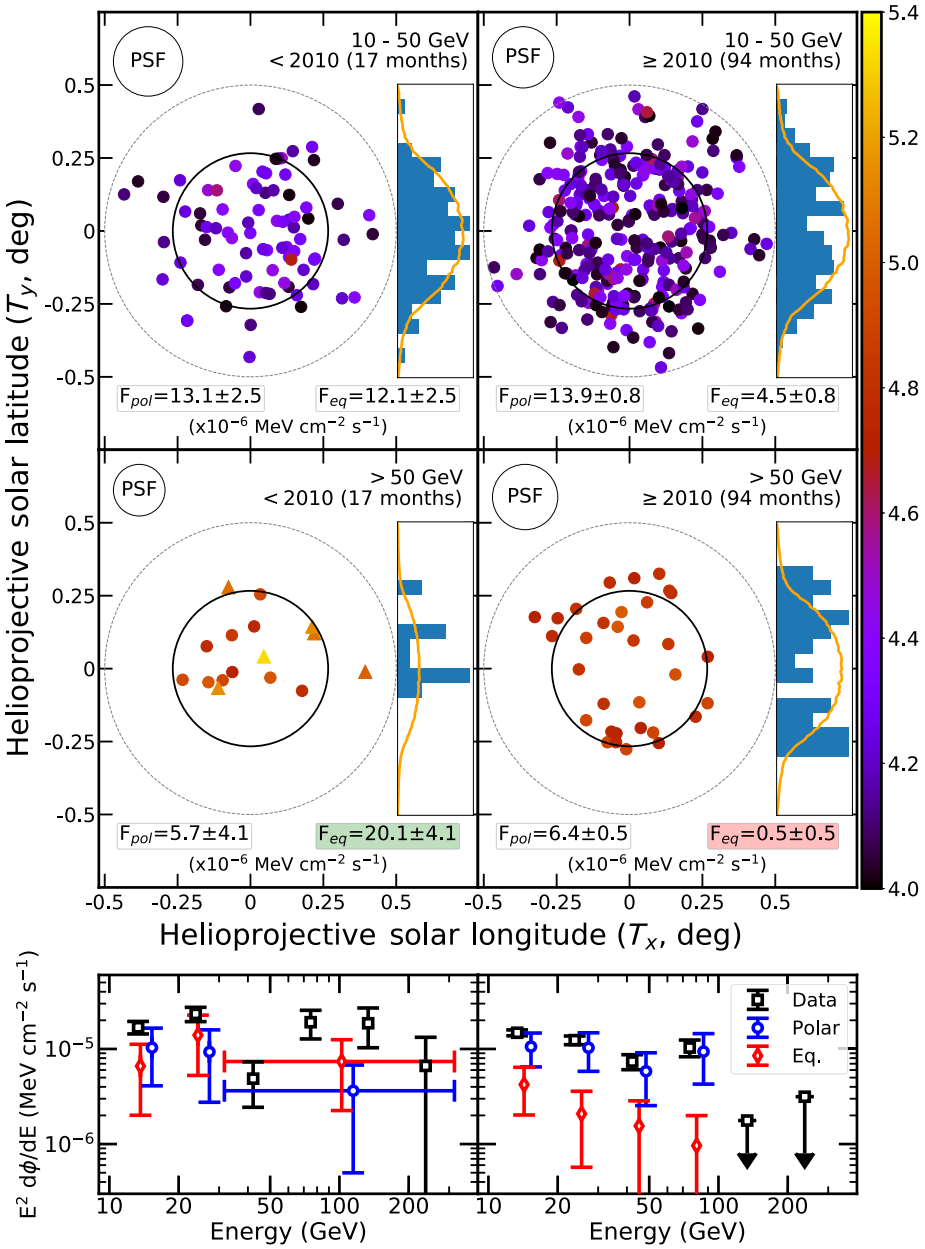

FIG. 2. (Top panel) The location and energy of solar γ rays in helioprojective coordinates. Data are cut into two temporal and two energy bins. The solid disk indicates the solar circle, and the dashed circle indicates the 0.5° ROI. The average 68% containment region of γ rays in each bin is depicted at the top left. The histogram depicts the T_y positions of photons compared to the expectation from isotropic solar emission smeared by the PSF (orange line). Events > 100 GeV are marked with triangles rather than circles. We stress that the exposure after solar minimum significantly exceeds the exposure during solar minimum. Thus, the observed number of counts does not indicate the relative flux. In each bin, we report the flux from the modeled polar and equatorial components, as described in the text. (Bottom panel) The energy spectrum of polar and equatorial emission, divided into regions during (left) and after (right) solar minimum. The polar emission is approximately constant, while the equatorial emission decreases drastically after solar minimum.

minimum. However, the amplitude of this shift increases significantly at high energies. (b) The morphological shift is produced by a significant decrease in the equatorial flux after solar minimum, while the polar flux remains relatively constant. Most significantly, at energies >50 GeV, the equatorial fluxes during and after solar minimum are inconsistent at 4.7σ.

In Fig. 2, we also show the polar and equatorial spectra during and after solar minimum. While the polar emission spectrum remains relatively constant, the equatorial spectrum softens substantially after solar minimum. This significantly decreases the high-energy equatorial flux after solar minimum, despite the similar normalization of the equatorial component at low energies. Intriguingly, the equatorial γ-ray

TABLE I. Event information for P8R2_SOURCE_V2 events with recorded energies exceeding 100 GeV observed within 0.5° of the solar center. Check marks indicate events that were recorded as photons in previous Pass 6 and 7 analyses, while "BG prob" indicates the probability that diffuse emission produced the event. Events below the extra space did not pass our default selection criteria, as they were observed when the Sun was located within 5° of the Galactic plane. (Additional event information is provided in Appendix J of the SM [31].)

Date	E (GeV)	Distance	Event class	$P6$	$P7$	BG prob
11/9/2008	212.8	0.068°	UltraCleanVeto	✓	✓	0.000 50
12/13/2008	139.3	0.126°	UltraCleanVeto	×	×	0.000 38
12/13/2008	103.3	0.399°	UltraCleanVeto	×	×	0.000 52
3/22/2009	117.2	0.255°	UltraCleanVeto	✓	✓	0.000 27
8/15/2009	138.5	0.261°	UltraCleanVeto	✓	✓	0.000 21
11/20/2009	112.6	0.288°	UltraCleanVeto	×	×	0.000 20
12/24/2008	226.9	0.069°	UltraClean	×	×	0.001 28
12/20/2009	467.7	0.338°	UltraCleanVeto	×	×	0.002 08

spectrum during solar minimum is extremely hard, and it is consistent with $dN/dE \sim E^{-2}$ up to energies exceeding 100 GeV. We note that we have combined high-energy spectral bins during solar minimum to improve the statistical separation of polar and equatorial components.

Flux above 100 GeV.—In Fig. 1, we discovered a bright γ-ray flux above 100 GeV during solar minimum, but we found no events in the remaining solar cycle. In Table I, we examine each >100 GeV event. We uncover no significant concerns regarding the event classes, or angular and energy reconstructions. All six events pass the UltraCleanVeto event cut, providing the highest confidence that they are γ rays. We calculate the probability that each event has a nonsolar origin by calculating the γ-ray flux above 100 GeV in each ROI during periods when the Sun is not present. We find that diffuse contributions cannot explain these events. The diffuse γ-ray flux above 100 GeV over the solar path produces $\sim$0.3 background events over the full analysis period (see Appendix C of the SM [31]).

Examining each event yields three insights. First, we observe several extremely high-energy events, including three events exceeding 200 GeV and one event at 470 GeV. The average Fermi-LAT energy dispersion near 100 GeV is $\sim$7%, indicating that these events have true energies well above 100 GeV. This suggests that multi-TeV protons can produce outgoing γ rays through solar interactions, and that HAWC observations of the upcoming solar minimum may be illuminating. In Fig. 5 of Ref. [18], we carefully compare the solar minimum flux against projected HAWC sensitivities.

Second, all six high-energy events were observed between November 2008 and November 2009, which is inconsistent with a steady-state hypothesis. We determine the significance of this variability by conducting a Kolmogorov-Smirnov test of the hypothesis that the data are Poissonian in solar exposure. We rule out the steady-state hypothesis at 4.2σ. Noting that the Sun moves through the Galactic plane during solar minimum and that the diffuse contribution along the plane is negligible above 100 GeV, we unblind the region $b < 5°$. This adds two new events above 100 GeV that were also observed at solar minimum, and no additional events during the subsequent eight passages of the Galactic plane. Including these events increases the statistical significance for variability to 4.9σ.

Third, we note a peculiar "double event" on December 13, 2008, when two >100 GeV γ rays were observed within 3.5 h. The probability that any two events are this closely correlated is inconsistent with Poissonian expectations at $\sim 2.9\sigma$.

Interpretation.—We have provided several lines of evidence that reveal two distinct γ-ray emission components on the solar disk. The first emits primarily from the Sun's polar regions, has a constant amplitude over the solar cycle, and produces no observed flux above 100 GeV. The second emits primarily from the Sun's equatorial plane, has an amplitude that decreases drastically after solar minimum, and has a hard spectrum at solar minimum that extends above 200 GeV.

These results are not explained by the SSG model. The bright γ-ray flux across the solar surface does support the SSG mechanism of cosmic-ray reversal deep within the photosphere. However, the flux, spectrum, time variation, morphological shift, and spectral dip of solar γ rays are unexplained. We can qualitatively parametrize the solar γ-ray flux as

$$\Phi_\odot(E_\gamma) = \frac{R_\odot^2}{4D^2} I_{\rm CR}(E_{\rm CR}) C(E_\gamma, E_{\rm CR}) f_{\rm sur} f_{\rm turn} f_{\rm int}, \quad (1)$$

where $\Phi_\odot$ is the disk γ-ray flux, $I_{\rm CR}$ is the cosmic-ray flux at the solar surface, C describes the γ-ray flux at energy E_γ produced by a hadronic interaction at energy $E_{\rm CR}$ (see Appendix E of the SM [31]), $f_{\rm sur}$ is the fraction of the solar surface that produces γ rays, $f_{\rm turn}$ is the fraction of incoming cosmic rays that are reversed by magnetic fields within the solar photosphere, and $f_{\rm int}$ is the fraction of these cosmic rays that undergo a hadronic interaction and produce outgoing γ rays before leaving the surface. SSG found solar modulation to be negligible, implying that $I_{\rm CR}$ is similar to the interstellar cosmic-ray flux. SSG assumes that each efficiency term is energy, position, and time independent. In particular, SSG set $f_{\rm sur}$ and $f_{\rm turn}$ to unity and calculated $f_{\rm int} \sim 0.5\%$.

Our observations instead indicate that these parameters strongly depend on the cosmic-ray energy, solar cycle, and solar latitude. At solar minimum, these shifts are remarkable for four reasons. The large flux, within a factor of $\sim$4 of the maximal value, implies that all efficiency parameters are near unity. The hard spectrum, significantly exceeding the $E^{-2.7}$ interstellar cosmic-ray spectrum, indicates that these efficiencies rise quickly with energy. The equatorial morphology indicates that polar regions are not emitting

efficiently, implying that $f_{\rm sur} \lesssim 0.5$. Finally, symmetry constrains $f_{\rm int} \sim 0.5$, as cosmic rays should undergo equal interactions while entering and exiting the photosphere. These considerations produce significant tension with any SSG-like model.

This tension motivates us to consider scenarios that violate the assumptions of Eq. (1) and allow for larger γ-ray fluxes. In Appendix K of the SM [31], we discuss the potential for effects such as magnetic focusing, cosmic-ray trapping, or anisotropic emission to boost the observed γ-ray flux. However, we find that each possibility is either observationally excluded or theoretically unmotivated.

One potential insight stems from the two >100 GeV γ rays observed on December 13, 2008, which may be connected to a contemporaneous Earth-bound coronal mass ejection (CME) that began on December 12, 2008 and encountered Earth on December 17 [47–49]. However, none of the remaining >100 GeV γ rays correspond to significant CMEs. In Appendix K of the SM [31], we discuss the potential for CMEs, helmet streamers, and coronal holes to explain the peculiar morphology and temporal variability of >100 GeV events.

A new event.—Recently, we found a new >100 GeV event. Observed on February 13, 2018, at 17:49:15 UTC, it has an energy of 162 GeV, is located 0.36° from the solar center, passes the UltraCleanVeto event selection, and belongs to the PSF0 and EDISP3 event classes. As we reenter solar minimum, this is the first >100 GeV event recorded within 0.5° of the Sun since 2009. It may be connected to an Earth-bound CME observed on February 12, 2018 [50]. Preliminary work indicates that this event increases the significance of the >100 GeV time variability above 5σ, and it supports the hypothesis that the upcoming solar minimum will provide a substantial flux of high-energy events.

Future outlook.—We have discovered statistically significant temporal variations in the intensity, spectrum, and morphology of solar γ-ray emission. These variations strongly suggest that two distinct components substantially contribute to the total solar γ-ray flux, including (1) a polar component that varies moderately in time and has a γ-ray spectrum that falls sharply around 100 GeV, and (2) an equatorial component with an extremely hard γ-ray spectrum that continues above 200 GeV but is dominant only during solar minimum. These observations provide important new clues about the mechanisms behind solar disk γ-ray emission, which remains mysterious.

This mystery is deepened by the high intensity and hard spectrum of disk emission. In particular, the solar minimum flux appears to be in tension with the most optimistic predictions from the class of models that convert the interstellar cosmic-ray flux into a time-invariant and isotropic γ-ray flux. If future observations detect emission at even moderately higher energies, a new mechanism will be necessary to explain the highest-energy solar emission.

Observations of the upcoming cycle 25 solar minimum by both Fermi-LAT and HAWC will provide valuable information. Preliminary estimates indicate that the cycle 25 minimum will be even quieter than the cycle 24 minimum [51]. Moreover, the Fermi-LAT satellite was operational only during the second half of the 2007–2009 cycle 24 minimum [16]. The observation of >100 GeV γ rays during this period will significantly enhance our understanding of high-energy solar disk γ-ray emission. One new event has recently been detected. With improved statistics, it will soon become possible to correlate γ rays with solar observables, shining light on the processes responsible for the high-energy γ-ray flux [31].

We thank Joe Giacalone, Dan Hooper, Igor Moskalenko, Nick Rodd, Andy Strong, and especially Keith Bechtol, Ofer Cohen, and Stuart Mumford for their helpful comments. This research makes use of SunPy, an open-source, community-developed solar analysis package [45]. T. L., B. Z., and A. H. G. P. are supported in part by NASA Grant No. 80NSSC17K0754. B. Z. is also supported by a University Fellowship from The Ohio State University. J. F. B. and B. Z. (partially) are supported by NSF Grant No. PHY-1714479. K. C. Y. N. is supported by the Croucher Fellowship and the Benoziyo Fellowship. T. Q. W. is supported by the Natural Science Foundation of China under Grant No. 11547029.

*linden.70@osu.edu; http://orcid.org/0000-0001-9888-0971
†zhou.1877@osu.edu; http://orcid.org/0000-0003-1600-8835
‡beacom.7@osu.edu; http://orcid.org/0000-0002-0005-2631
§apeter@physics.osu.edu; http://orcid.org/0000-0002-8040-6785
‖chun-yu.ng@weizmann.ac.il; http://orcid.org/0000-0001-8016-2170
¶qwtang@ncu.edu.cn; http://orcid.org/0000-0001-7471-8451

[1] R. J. Murphy, C. D. Dermer, and R. Ramaty, Astrophys. J. Suppl. Ser. **63**, 721 (1987).
[2] G. Kanbach, D. L. Bertsch, C. E. Fichtel, R. C. Hartman, S. D. Hunter, D. A. Kniffen, B. W. Hughlock, A. Favale, R. Hofstadter, and E. B. Hughes, Space Sci. Rev. **49**, 69 (1988).
[3] G. Kanbach, D. L. Bertsch, C. E. Fichtel, R. C. Hartman, S. D. Hunter, D. A. Kniffen, P. W. Kwok, Y. C. Lin, J. R. Mattox, and H. A. Mayer-Hasselwander, Astron. Astrophys. Suppl. Ser. **97**, 349 (1993).
[4] M. Ackermann *et al.* (Fermi-LAT Collaboration), Astrophys. J. **787**, 15 (2014).
[5] M. Pesce-Rollins, N. Omodei, V. Petrosian, W. Liu, F. R. da Costa, A. Allafort, and Q. Chen, Astrophys. J. **805**, L15 (2015).
[6] M. Ackermann *et al.* (Fermi-LAT Collaboration), Astrophys. J. **835**, 219 (2017).
[7] G. H. Share, R. J. Murphy, A. K. Tolbert, B. R. Dennis, S. M. White, R. A. Schwartz, and A. J. Tylka, arXiv:1711.01511.

[8] M. Ajello *et al.* (Fermi-LAT Collaboration), Astrophys. J. **789**, 20 (2014).

[9] A. A. Abdo, M. Ackermann, M. Ajello, L. Baldini, J. Ballet, G. Barbiellini, D. Bastieri, K. Bechtol *et al.*, Astrophys. J. **734**, 116 (2011).

[10] I. V. Moskalenko, T. A. Porter, and S. W. Digel, Astrophys. J. Lett. **652**, L65 (2006).

[11] E. Orlando and A. W. Strong, Astrophys. Space Sci. **309**, 359 (2007).

[12] E. Orlando, N. Giglietto, I. Moskalenko, S. Raino, and A. Strong, Proc. Sci., ICRC2017 (**2017**) 693 [arXiv:1712.09745].

[13] K. C. Y. Ng, J. F. Beacom, A. H. G. Peter, and C. Rott, Phys. Rev. D **94**, 023004 (2016).

[14] E. Orlando and A. W. Strong, Astron. Astrophys. **480**, 847 (2008).

[15] B. Zhou, K. C. Y. Ng, J. F. Beacom, and A. H. G. Peter, Phys. Rev. D **96**, 023015 (2017).

[16] J. T. Emmert, J. L. Lean, and J. M. Picone, Geophys. Res. Lett. **37**, L12102 (2010).

[17] D. Seckel, T. Stanev, and T. K. Gaisser, Astrophys. J. **382**, 652 (1991).

[18] Q.-W. Tang, K. C. Y. Ng, T. Linden, B. Zhou, J. F. Beacom, and A. H. G. Peter, arXiv:1804.06846 [Phys. Rev. D (to be published)].

[19] W. B. Atwood *et al.* (Fermi-LAT Collaboration), Astrophys. J. **697**, 1071 (2009).

[20] A. U. Abeysekara *et al.*, Astropart. Phys. **50–52**, 26 (2013).

[21] M. G. Aartsen *et al.* (IceCube Collaboration), Phys. Rev. Lett. **110**, 131302 (2013).

[22] B. Batell, M. Pospelov, A. Ritz, and Y. Shang, Phys. Rev. D **81**, 075004 (2010).

[23] P. Schuster, N. Toro, and I. Yavin, Phys. Rev. D **81**, 016002 (2010).

[24] P. Meade, S. Nussinov, M. Papucci, and T. Volansky, J. High Energy Phys. 06 (2010) 029.

[25] N. F. Bell and K. Petraki, J. Cosmol. Astropart. Phys. 04 (2011) 003.

[26] J. L. Feng, J. Smolinsky, and P. Tanedo, Phys. Rev. D **93**, 115036 (2016); **96**, 099903(E) (2017).

[27] R. K. Leane, K. C. Y. Ng, and J. F. Beacom, Phys. Rev. D **95**, 123016 (2017).

[28] C. A. Argelles, G. de Wasseige, A. Fedynitch, and B. J. P. Jones, J. Cosmol. Astropart. Phys. 07 (2017) 024.

[29] J. Edsjo, J. Elevant, R. Enberg, and C. Niblaeus, J. Cosmol. Astropart. Phys. 06 (2017) 033.

[30] K. C. Y. Ng, J. F. Beacom, A. H. G. Peter, and C. Rott, Phys. Rev. D **96**, 103006 (2017).

[31] See Supplemental Material at http://link.aps.org/supplemental/10.1103/PhysRevLett.121.131103, which includes Refs. [32–44], for further information regarding the extraction of the solar emission described in this analysis.

[32] S. Agostinelli *et al.* (GEANT4 Collaboration), Nucl. Instrum. Methods Phys. Res., Sect. A **506**, 250 (2003).

[33] L. F. Burlaga, N. F. Ness, Y.-M. Wang, and N. R. Sheeley, J. Geophys. Res.: Space Phys. **107**, 1410 (2002).

[34] R. D. Strauss, M. S. Potgieter, I. Büsching, and A. Kopp, Astrophys. Space Sci. **339**, 223 (2012).

[35] I. Cholis, D. Hooper, and T. Linden, Phys. Rev. D **93**, 043016 (2016).

[36] N. Gopalswamy, S. Yashiro, and S. Akiyama, Astrophys. J. Lett. **823**, L15 (2016).

[37] M. Amenomori *et al.* (Tibet ASγ Collaboration), Phys. Rev. Lett. **111**, 011101 (2013).

[38] R. M. E. Illing and A. J. Hundhausen, J. Geophys. Res. **90**, 275 (1985).

[39] O. Panasenco, S. Martin, A. D. Joshi, and N. Srivastava, J. Atmos. Sol. Terr. Phys. **73**, 1129 (2011).

[40] N. Gopalswamy, M. Shimojo, W. Lu, S. Yashiro, K. Shibasaki, and R. A. Howard, Astrophys. J. **586**, 562 (2003).

[41] S. Yashiro, N. Gopalswamy, G. Michalek, O. C. St. Cyr, S. P. Plunkett, N. B. Rich, and R. A. Howard, J. Geophys. Res.: Space Phys. **109**, A07105 (2004).

[42] B. C. Low, Sol. Phys. **167**, 217 (1996).

[43] E. Endeve, T. E. Holzer, and E. Leer, Astrophys. J. **603**, 307 (2004).

[44] K. Fujiki, M. Tokumaru, K. Hayashi, D. Satonaka, and K. Hakamada, Astrophys. J. Lett. **827**, L41 (2016).

[45] S. J. Mumford, S. Christe, D. Pérez-Suárez, J. Ireland, A. Y. Shih, A. R. Inglis, S. Liedtke, R. J. Hewett, F. Mayer, K. Hughitt, N. Freij, T. Meszaros, S. M. Bennett, M. Malocha, J. Evans, A. Agrawal, A. J. Leonard, T. P. Robitaille, B. Mampaey, J. I. Campos-Rozo *et al.* (SunPy Community), Comput. Sci. Discovery **8**, 014009 (2015).

[46] T. P. Robitaille, E. J. Tollerud, P. Greenfield, M. Droettboom, E. Bray, T. Aldcroft, M. Davis, A. Ginsburg, A. M. Price-Whelan, W. E. Kerzendorf, A. Conley, N. Crighton, K. Barbary, D. Muna, H. Ferguson, F. Grollier, M. M. Parikh, P. H. Nair, H. M. Günther, C. Deil *et al.* (Astropy Collaboration), Astron. Astrophys. **558**, A33 (2013).

[47] J. P. Byrne, S. A. Maloney, R. T. J. McAteer, J. M. Refojo, and P. T. Gallagher, Nat. Commun. **1**, 74 (2010).

[48] J. P. Byrne, Ph.D. thesis, Trinity College Dublin, 2012.

[49] C. E. DeForest, T. A. Howard, and D. J. McComas, Astrophys. J. **769**, 43 (2013).

[50] See https://www.swpc.noaa.gov/news/c1-flare-and-associated-cme-12-february-2018.

[51] D. H. Hathaway and L. A. Upton, J. Geophys. Res.: Space Phys. **121**, 10 (2016).